

The Confining Interaction and Radiative Decays of Heavy Quarkonia

T.A. Lähde*, C.J. Nyfält† and D.O. Riska‡

*Department of Physics
POB 9, 00014 University of Helsinki
Finland*

Abstract

The radiative spin-flip transition rates of heavy quarkonium states depend sensitively on the matrix elements of the effective confining interaction through the associated two-quark exchange current operator. The Hamiltonian model based on a scalar linear confining interaction with a single gluon exchange hyperfine term is shown to provide an adequate description of the $J/\psi \rightarrow \eta_c \gamma$ and $\psi(2S) \rightarrow \eta_c \gamma$ decay widths once the relativistic single quark magnetic moment operator is treated without approximation and the exchange current is taken into account. Predictions are given for the radiative spin-flip decay widths of the $1S, 2S$ and $3S$ states of the $c\bar{c}$, $b\bar{b}$ and B_c^+ systems. In the B_c^+ system the gluon exchange current also contributes to the spin-flip transition rates.

*talahde@rock.helsinki.fi

†nyfalt@rock.helsinki.fi

‡riska@rock.helsinki.fi

1 Introduction

The spectra of the $c\bar{c}$ and $b\bar{b}$ meson systems are fairly well reproduced by a Schrödinger equation based description with an interaction Hamiltonian formed of a scalar linear confining interaction and a single gluon exchange model for the hyperfine interaction [1, 2]. This model is qualitatively supported by numerical construction of the effective interaction by lattice methods [3, 4]. For this linear confinement + gluon exchange model the parameter freedom has recently been narrowed considerably by numerical precision determination of the effective quark-gluon coupling strength α_s [5, 6].

While the spectra of the $c\bar{c}$ and $b\bar{b}$ systems are fairly well accounted for by the simple linear confinement + gluon exchange interaction model, the situation concerning the radiative widths of the spin-flip transitions $J/\psi \rightarrow \eta_c \gamma$ and $\psi(2S) \rightarrow \eta_c \gamma$ has remained unsettled [7, 8, 9]. We show here that these radiative transitions strengths are in fact also satisfactorily described by the conventional quantum mechanical framework, provided that the full Dirac structure of the quark current operators is taken into account along with the exchange current operator that is generated by coupling to intermediate negative energy states by the linear scalar confining operator Fig.1, once the same Hamiltonian is used to generate both the wave functions and the current operators. This exchange current contribution is decisive for achieving agreement between the calculated and measured M1 transition rates of the J/ψ and the ψ' . The exchange current operator is required by current conservation with the confining interaction.

The contribution of the exchange current operator that is associated with the linear potential is essential for reproduction of the empirical decay widths. Moreover this operator only arises under the assumption that the effective confining interaction is a Lorentz scalar (“S”), which supports the consistency requirement of ref.[10]. If the Lorentz invariant structure of the confining interaction were a vector invariant (“V”), the associated exchange current operator would contain no spin-flip term when the quark and anti-quarks have equal mass as in the $c\bar{c}$ system, and agreement with the empirical decay widths would be excluded.

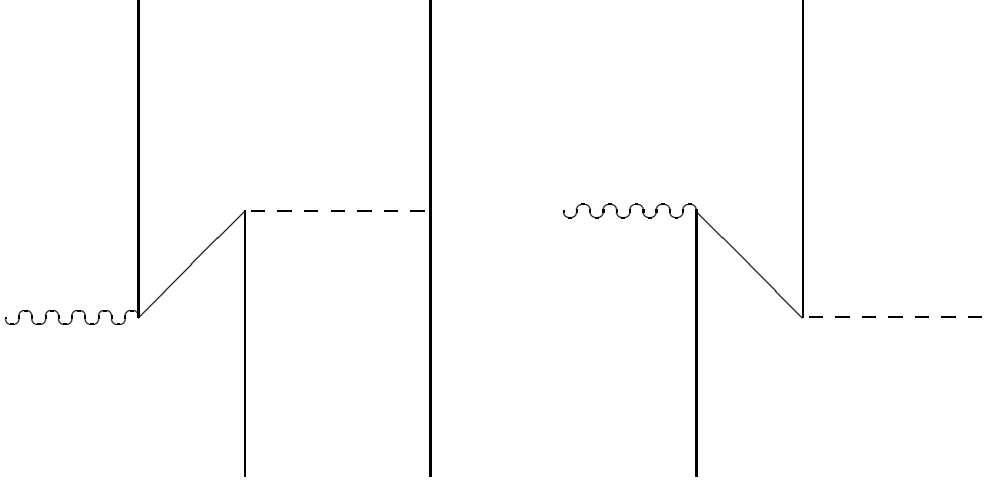


Figure 1: Exchange current operators associated with the effective scalar confining and gluon exchange interactions, with intermediate virtual $q\bar{q}$ excitations.

In the case of the B_c^+ system, the first state of which has recently been observed [11], the exchange current that is associated with the vector gluon exchange interaction in contrast also contains a component that is antisymmetric in the spins of the quarks and antiquarks, which in this case have unequal mass. That exchange current consequently also plays a role in the spin-flip transitions of the B_c^+ system, because of the large difference in mass between the c and b quarks. The role of these exchange currents is shown here by a calculation of the decay widths for the radiative spin-flip transitions $B_c^+(J = 1, nS) \rightarrow B_c^+(J = 0, 1S)\gamma$ ($n = 1, 2, 3$). The decay widths are calculated here with full account of both the confinement and gluon exchange currents. The radiative decay widths have been calculated in the non-relativistic impulse approximation without consideration of the exchange current contributions in ref.[12]. Experimental determination of these decay widths should be decisive for settling the quantitative importance of the exchange current operators and the validity of the present phenomenological approach to the structure of heavy quarkonia.

The B_c^+ systems differ from the $c\bar{c}$ and $b\bar{b}$ systems also in that the B_c^+ meson have magnetic moments. These also obtain considerable exchange current contributions which are calculated here.

The framework used here is similar to that employed in refs. [7, 8] for the calculation of the rates of the M1 transitions in the $c\bar{c}$ and $b\bar{b}$ systems. The affirmative conclusion about the significance of the exchange current contributions here is new. The numerical values differ from those in refs.[7, 8] partly because the unapproximated Dirac magnetic moment operator is considered here, and because of an overestimate of the lowest order relativistic correction to the quark magnetic moment operator.

This paper is divided into 5 sections. In section 2 we describe the Hamiltonian model for the heavy quarkonium systems, and demonstrate that it describes the spectra of the $c\bar{c}$ and $b\bar{b}$ mesons satisfactorily. In section 2.3 we show the predicted spectrum of the B_c^+ system. In section 3 we describe the model for the current operator for the heavy quarkonium system. The corresponding calculated decay widths for the radiative spin-flip transitions of the $c\bar{c}$, $b\bar{b}$ and B_c^+ mesons are presented in section 4. Finally section 5 contains a concluding discussion.

2 Model Hamiltonian

2.1 Hamiltonian

The linear scalar confinement + gluon exchange hyperfine interaction Hamiltonian model for heavy quarkonia $Q\bar{q}$, is formed of quarks Q and antiquarks \bar{q} with in general unequal mass

$$H = H_{kin} + V_C + V_G \quad (1)$$

where H_{kin} is the kinetic energy term and V_C and V_G are the potentials that describe the confining and gluon exchange interactions respectively.

The kinetic energy term, which in heavy quark effective theory is taken to include the terms to order m^{-4} is

$$H_{kin} = m_Q + m_{\bar{q}} + \frac{p^2}{2m_r} - \frac{1}{8} \left(\frac{m_Q^3 + m_{\bar{q}}^3}{m_Q^3 m_{\bar{q}}^3} \right) p^4, \quad (2)$$

where m_r is the reduced mass $m_r = m_Q m_{\bar{q}} / (m_Q + m_{\bar{q}})$ and \vec{p} is the relative momentum. The term of $\mathcal{O}(p^4)$, which will be treated as a perturbation increases in importance with excitation number, and is non-negligible because of the compact spatial extent of the confined quarkonium wave functions.

The scalar confining potential has the form (to order m^{-2}):

$$V_C(r) = cr \left\{ 1 - \frac{\vec{p}^2}{2} \frac{m_Q^2 + m_{\bar{q}}^2}{m_Q^2 m_{\bar{q}}^2} \right\} - \frac{c}{4r} \frac{m_Q^2 + m_{\bar{q}}^2}{m_Q^2 m_{\bar{q}}^2} \vec{S} \cdot \vec{L} \\ + \frac{c}{8r} \frac{m_Q^2 - m_{\bar{q}}^2}{m_Q^2 m_{\bar{q}}^2} (\vec{\sigma}_Q - \vec{\sigma}_{\bar{q}}) \cdot \vec{L}. \quad (3)$$

The last antisymmetric spin-orbit term in this interaction vanishes for equal mass quarkonia.

The single gluon exchange interaction potential to order m^{-2} has the form

$$V_G(r) = -\frac{4}{3} \alpha_s \left\{ \frac{1}{r} - \pi \delta^{(3)}(\vec{r}) \frac{m_Q^2 + m_{\bar{q}}^2}{2m_Q^2 m_{\bar{q}}^2} + \frac{\vec{p}^2}{r m_Q m_{\bar{q}}} \right\} \\ + \frac{8\pi}{9} \frac{\alpha_s}{m_Q m_{\bar{q}}} \delta^{(3)}(\vec{r}) \vec{\sigma}^1 \cdot \vec{\sigma}^2 + \frac{\alpha_s}{3m_Q m_{\bar{q}}} \frac{1}{r^3} S_{12} \\ + \frac{2\alpha_s}{3r^3} \left\{ \frac{m_Q^2 + m_{\bar{q}}^2}{2m_Q^2 m_{\bar{q}}^2} + \frac{2}{m_Q m_{\bar{q}}} \right\} \vec{S} \cdot \vec{L} + \frac{\alpha_s}{6r^3} \frac{m_Q^2 - m_{\bar{q}}^2}{m_Q^2 m_{\bar{q}}^2} (\vec{\sigma}_Q - \vec{\sigma}_{\bar{q}}) \cdot \vec{L}. \quad (4)$$

Here $S_{12} \equiv 3\vec{\sigma}_Q \cdot \hat{r} \vec{\sigma}_{\bar{q}} \cdot \hat{r} - \vec{\sigma}_Q \cdot \vec{\sigma}_{\bar{q}}$ is the usual tensor interaction operator.

The interaction operator constructed to order m^{-2} by lattice methods in refs. [3, 4] contains in addition to the operators of the form contained in the model Hamiltonian (1) that involve the non-local operator \vec{p}/m to second order, but which do not significantly affect the calculated spectra. We do not include such here, mainly because they lack an immediate dynamical interpretation. The interaction operator derived in refs. [3, 4] has a string tension c of ~ 1.1 GeV/fm, with a slight flavor dependence.

	$c\bar{c}$	B_c^+	$b\bar{b}$
\mathbf{c}	1.11 GeV/fm	1.11 GeV/fm	1.11 GeV/fm
α_s	0.40	0.32	0.29
\mathbf{m}_c	1.48 GeV	1.48 GeV	–
\mathbf{m}_b	–	4.72 GeV	4.72 GeV

Table 1: Parameter values for the model Hamiltonian (1) used here.

We shall here use parameter values close to those suggested in [3, 4, 6], but determine the precise values by phenomenological fits to the $c\bar{c}$ and $b\bar{b}$ spectra. The values used are listed in Table 1. The values for the color fine structure constant α_s in the table are close to those obtained by lattice methods in refs. [5, 6]: $\alpha_s = 0.38$ at the charmonium scale $m_c \sim 1.3$ and $\alpha_s = 0.22$ at the bottom scale $m_b \sim 4.1$ GeV respectively. These values agree well with the inverse logarithmic momentum dependence predicted by perturbative *QCD*. The phenomenologically determined quark masses in Table 1 should be viewed as constituent quark masses. The overall description of the empirical spectra corresponds to that achieved in refs. [3, 4].

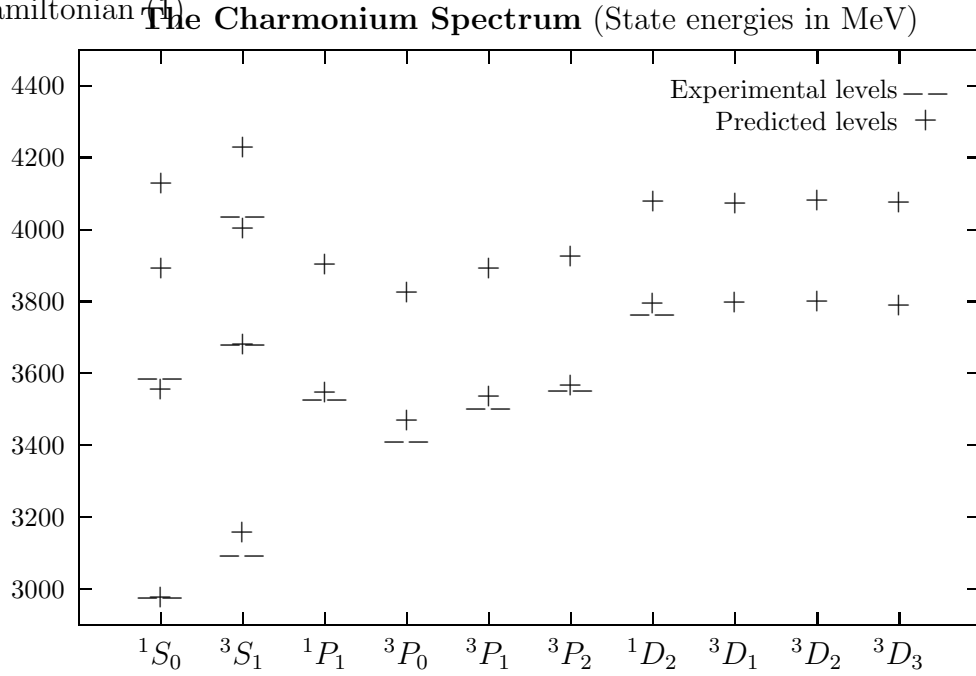
2.2 The $c\bar{c}$ and $b\bar{b}$ Spectra

The calculated spectra for the $c\bar{c}$ and $b\bar{b}$ systems that are obtained by solving the Schrödinger equation for the model Hamiltonian (1) are shown in Figs. 2 and 3 respectively. In the calculation the term of order p^4 in the kinetic energy operator (2), as well as all the terms of order m^{-2} in the interaction potentials V_c (3) and V_G (4) were treated in first order perturbation theory. The parameter values used were those in Table 1, which are close to those employed in ref. [12]. The perturbative treatment is motivated by the fact that the main focus here will be the calculation of the radiative widths of the *S*-states, for which the only terms in the fine structure part of the interaction that matter are the delta function terms in (3) and (4), which have to be treated perturbatively.

state	$\mathbf{s} = \mathbf{0}$ $j = l$	$j = l - 1$	$\mathbf{s} = \mathbf{1}$ $j = l$	$j = l + 1$
1S	2978 (2979)		3159 (3097)	
2S	3558 (3594)		3683 (3686)	
3S	3895		4004	
4S	4130		4231	
1P	3547 (3526)	3471 (3415)	3538 (3511)	3567 (3556)
2P	3903	3827	3892	3926
1D	3796	3798	3802	3790
2D	4079	4075	4083	4077

Table 2: The $c\bar{c}$ -states in MeV.

Figure 2: Charmonium spectrum with $m_c = 1480$ MeV obtained from the Hamiltonian $H^{(1)}$



state	s = 0 $j = l$	$j = l - 1$	s = 1 $j = l$	$j = l + 1$
1S	9411		9490 (9460)	
2S	9964		10008 (10023)	
3S	10311		10346 (10345)	
4S	10589		10621	
1P	9895	9868 (9860)	9890 (9892)	9903 (9913)
2P	10248	10224 (10232)	10243 (10255)	10256 (10268)
1D	10138	10135	10138	10140
2D	10435	10431	10435	10438

Table 3: The $b\bar{b}$ -states in MeV.

The quality of the agreement between the calculated and empirical $c\bar{c}$ and $b\bar{b}$ spectra in Figs. 2 and 3 is similar to that of the corresponding spectra obtained by the full numerically constructed Hamiltonian model [3, 4]. In both cases the splitting between the lowest S -states (η_c , J/ψ) is overpredicted and that of the P -states (χ_{cJ}) is somewhat underpredicted. A better description of the $\eta_c - J/\psi$ splitting may be obtained with the Buchmüller-Tye potential [13] used in ref. [2], but only at the price of underprediction of the excited states. This problem appears to be generic to Hamiltonian models of the type (1). The calculated spectra are nevertheless in good overall agreement with the empirical spectra, with hyperfine splittings of the multiplets which are ordered as the empirical ones. The model therefore appears realistic enough for a quantitative calculation of the spectrum of the B_c^+ system as well [12].

In Fig. 2 the empirical $c\bar{c}$ state at 4160 MeV has been given the assignment 4^3S_1 state, although it may be a $2D$ state [14]. Similarly the empirical Υ state at 10580 MeV has been given the assignment 4^3S_1 in Fig. 3. These states fall sufficiently low for this assignment with the present model, mainly as a consequence of the p^2 term in the effective confining interaction (3).

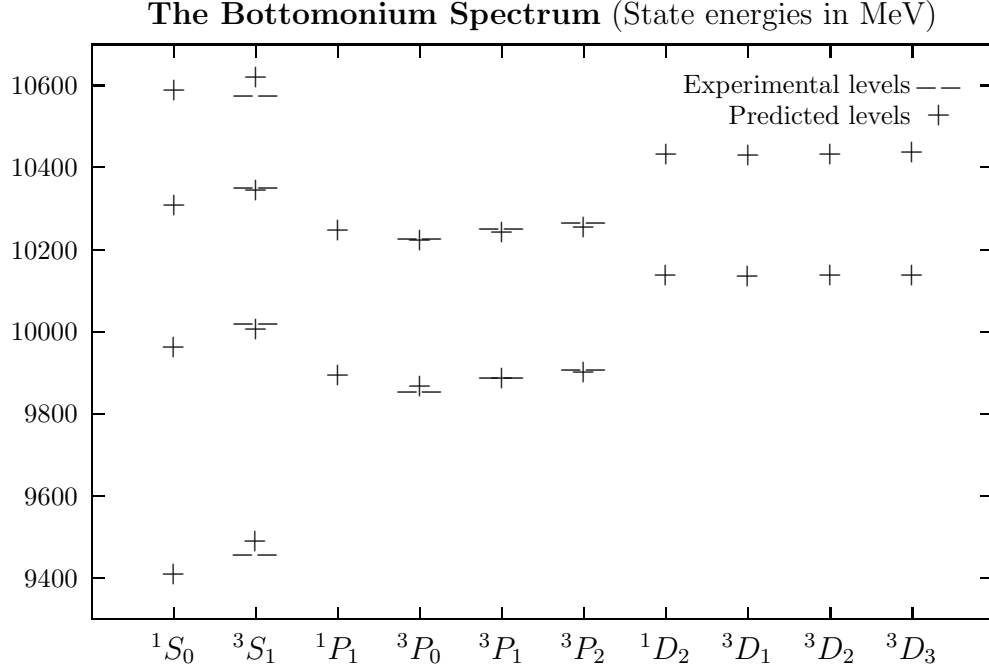


Figure 3: Bottomonium spectrum with $m_b = 4720$ MeV obtained from the Hamiltonian (1)

2.3 The B_c^+ Meson Spectrum

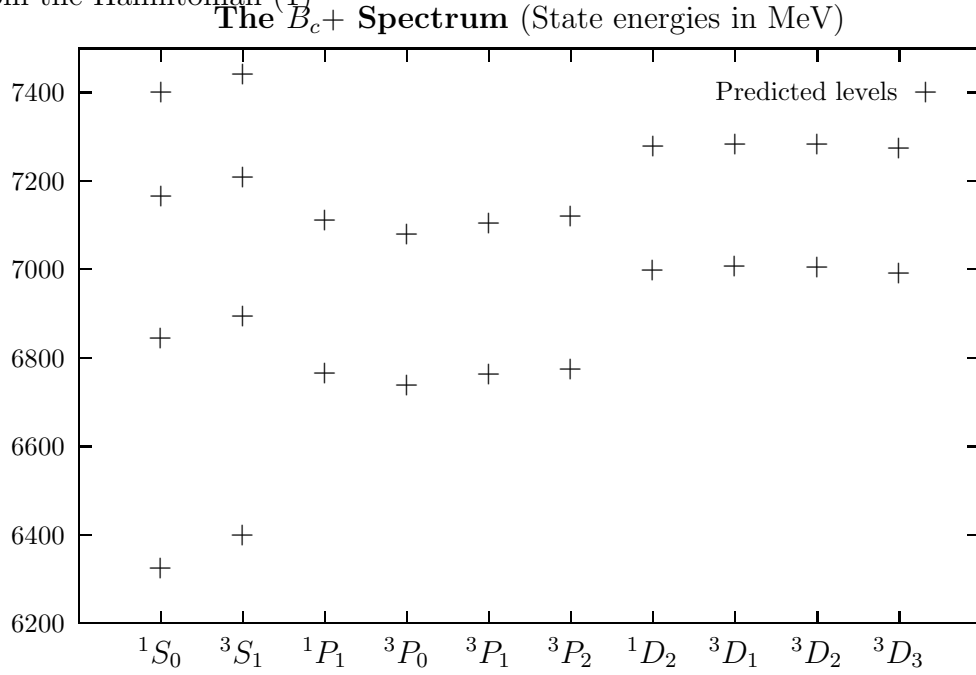
The first state of the B_c^+ meson spectrum, formed of c and \bar{b} quarks - presumably a 1^3S_1 -state - has recently been observed [11]. The Hamiltonian model (1) may be applied directly to the calculation of the spectrum of the B_c^+ system. By setting $\alpha_s = 0.32$ the $1S$ -states agree with the earlier spectra calculated in ref.[2]. The precise value for the empirical mass of the discovered B_c^+ -state is not yet known.

The predicted B_c^+ meson spectrum is shown in Fig. 4. This overall feature of this spectrum is that of an interpolation between the spectra of the $c\bar{c}$ and the $b\bar{b}$ systems. The large mass difference between the c and b quarks brings no qualitatively new features, although it does lead to the antisymmetric spin-orbit interactions in (3) and (4).

state	s = 0 $j = l$	$j = l - 1$	s = 1 $j = l$	$j = l + 1$
1S	6330		6404	
2S	6850		6900	
3S	7171		7214	
4S	7408		7448	
1P	6772	6743	6769	6779
2P	7116	7086	7111	7125
1D	7005	7013	7010	6998
2D	7284	7288	7288	7280

Table 4: The B_c^+ -states in MeV.

Figure 4: B_c^+ spectrum with $m_c = 1480$ MeV and $m_b = 4720$ MeV obtained from the Hamiltonian (1)



The predicted energy values in Table 4 and in Fig. 4 agree fairly well with those obtained in ref.[12], although the major shell spacings here are somewhat smaller, a feature that was built in because that is in better agreement with the empirical $c\bar{c}$ and $b\bar{b}$ spectra.

3 The Current Operator

3.1 Single Quark Current

Under the assumption that the b and c quarks are point Dirac particles, their current density operators have the form

$$\langle p' | \vec{j}(0) | p \rangle = iQe\bar{u}(p')\vec{\gamma}u(p), \quad (5)$$

where Q is the quark charge factor (+2/3, -1/3 respectively). Assuming canonical boosts for the spinors u, \bar{u} , the spin part of the current (5) yields the following magnetic moment operator [15]:

$$\vec{\mu} = Q \left(\frac{m_p}{m_Q} \right) \frac{\vec{\sigma}_Q}{\sqrt{1 + \vec{v}^2}} \left\{ 1 - \frac{1}{3} \left(1 - \frac{1}{\sqrt{1 + \vec{v}^2}} \right) \right\} \mu_N. \quad (6)$$

Here \vec{v} is the quark velocity $\vec{v} = (\vec{p}' + \vec{p})/2m_Q$, m_p is the proton mass and μ_N is the nuclear magneton.

For the $c\bar{c}$ and $b\bar{b}$ systems the spin-magnetic moments (6) combine to a spin-flip term of the form

$$\vec{\mu}_1 = \left(\frac{2}{3}, -\frac{1}{3} \right) \left(\frac{m_p}{m_Q} \right) \frac{\vec{\sigma}_Q - \vec{\sigma}_{\bar{Q}}}{\sqrt{1 + \vec{v}^2}} \left\{ 1 - \frac{1}{3} \left(1 - \frac{1}{\sqrt{1 + \vec{v}^2}} \right) \right\} \mu_N. \quad (7)$$

The matrix element of this operator for a spin-flip transition $J = 1 \leftrightarrow J = 0$ between S -states of the $c\bar{c}$ and $b\bar{b}$ system may be expressed as

$$\begin{aligned} \langle f | \vec{\mu}_1 | i \rangle &= 4 \left(\frac{2}{3}, -\frac{1}{3} \right) \left(\frac{m_p}{m_Q} \right) \mu_N \int_0^\infty dp p^2 \int_{-1}^1 dz \\ &\int_0^\infty dr' r'^2 \int_0^\infty dr r^2 \varphi_f(r') \frac{1}{\sqrt{1 + \vec{v}^2}} \left\{ 1 - \frac{1}{3} \left(1 - \frac{1}{\sqrt{1 + \vec{v}^2}} \right) \right\} \\ &j_0 \left(r' \left| \vec{p} + \frac{\vec{q}}{4} \right| \right) j_0 \left(r \left| \vec{p} - \frac{\vec{q}}{4} \right| \right) \varphi_i(r). \end{aligned} \quad (8)$$

Here $\vec{v} \equiv \vec{p}/m$, and $\varphi_i(r)$ and $\varphi_f(r')$ are the radial wave functions for the initial and final S -states.

The matrix element (8) would be considerably simplified by expansion to lowest order in \vec{v} of the square roots in the expression (6). This would however lead to misleading results as the radiative widths of the S -states are very sensitive to the model of the current operator and the wave functions [7]. For reference we note that if only the order $(v)^0$ term is kept in (7) the expression (8) reduces to the standard non-relativistic impulse approximation result

$$\langle f|\mu|i \rangle = \left(\frac{2}{3}, -\frac{1}{3}\right) \left(\frac{m_p}{m_Q}\right) \mu_N \int_0^\infty dr r^2 \varphi_f(r) j_0\left(\frac{qr}{2}\right) \varphi_i(r). \quad (9)$$

Here $Q = c, b$ for $c\bar{c}$ and $b\bar{b}$ respectively. The higher order terms in (8) lead to numerical values that differ significantly from this result as shown below.

If the magnetic moment expression (8) is expanded to second order in v^2 , the correction factor to the non-relativistic magnetic moment operator is $1 - 2v^2/3$. The coefficient $2/3$ in this bracket was obtained incorrectly as $5/6$ in refs. [7, 8], with a consequent overestimate of this relativistic correction. The factor $2/3$ is obtained as the sum of two terms, one of which arises from the normalization of the Dirac spinors $(1/2)$ [16] and another, which arises from the difference between the initial and final quark momenta $(1/6)$.

For the B_c^+ system the spin dependent part of the magnetic moment operator (7) is modified to

$$\begin{aligned} \vec{\mu}_1(B_c^+) = & \frac{1}{6} m_p (\vec{\sigma}_c + \vec{\sigma}_{\bar{b}}) \left\{ \frac{2}{m_c} \frac{1}{\sqrt{1 + \vec{v}_c^2}} \left[1 - \frac{1}{3} \left(1 - \frac{1}{\sqrt{1 + \vec{v}_c^2}} \right) \right] \right. \\ & + \frac{1}{m_b} \frac{1}{\sqrt{1 + \vec{v}_b^2}} \left[1 - \frac{1}{3} \left(1 - \frac{1}{\sqrt{1 + \vec{v}_b^2}} \right) \right] \left. \right\} \mu_N \\ & + \frac{1}{6} m_p (\vec{\sigma}_c - \vec{\sigma}_{\bar{b}}) \left\{ \frac{2}{m_c} \frac{1}{\sqrt{1 + \vec{v}_c^2}} \left[1 - \frac{1}{3} \left(1 - \frac{1}{\sqrt{1 + \vec{v}_c^2}} \right) \right] \right. \\ & - \frac{1}{m_b} \frac{1}{\sqrt{1 + \vec{v}_b^2}} \left[1 - \frac{1}{3} \left(1 - \frac{1}{\sqrt{1 + \vec{v}_b^2}} \right) \right] \left. \right\} \mu_N, \end{aligned} \quad (10)$$

where $\vec{v}_c \equiv \vec{p}/m_c$ and $\vec{v}_b \equiv \vec{p}/m_b$ respectively. The term that is symmetric in the spins gives rise to a magnetic moment for the 3S_1 state of the B_c^+ system, whereas the term that is antisymmetric in the spins gives rise to spin-flip transitions.

The radiative widths calculated using these single quark magnetic moments – the impulse approximation – do not agree with the presently known empirical rates for M1 transitions. These discrepancies can be considerably ameliorated, if not entirely eliminated, by taking into account the exchange current contributions.

3.2 Exchange Current Operators

The scalar confining interaction may excite virtual quark-antiquark states, which are deexcited by the external electromagnetic field. This process, which is illustrated by the Feynman diagrams in Fig. 1, generates an exchange current – or two-quark pair excitation current, which in the $c\bar{c}$ and $b\bar{b}$ system may, to order m^{-2} , be expressed in compact form as

$$\vec{j}_2(C) = -\frac{cr}{m_Q}\vec{j}_1, \quad (11)$$

where \vec{j}_1 is the corresponding single quark current operator. This exchange current operator is required to satisfy the continuity equation once the terms of order $1/m^2$ are included in the confining interaction (3).

The spin dependent part of the corresponding exchange magnetic moment operator is then, to lowest order in $1/m^2$, for the $c\bar{c}$ and $b\bar{b}$ systems:

$$\vec{\mu}_2(C) = -\left(\frac{2}{3}, -\frac{1}{3}\right) \frac{m_p}{m_Q} \frac{cr}{m_Q} (\vec{\sigma}_Q - \vec{\sigma}_{\bar{q}}) \mu_N, \quad (12)$$

where the factor $2/3$ in the bracket applies to the $c\bar{c}$ system and the factor $-1/3$ to the $b\bar{b}$ system and $m_Q = m_c$ and m_b respectively. The matrix element of this operator for a transition $i \rightarrow f + \gamma$ is then [7]

$$\langle f | \vec{\mu}_2(C) | i \rangle = -\left(\frac{2}{3}, -\frac{1}{3}\right) \frac{m_p}{m_Q^2} \mu_N \int_0^\infty dr r^2 \varphi_f(r) cr j_0\left(\frac{qr}{2}\right) \varphi_i(r). \quad (13)$$

The contributions of these matrix elements turn out to be essential for the explanation of the empirical decay widths of the transitions $J/\psi \rightarrow \eta_c \gamma$ and

$$\psi(2S) \rightarrow \eta_c \gamma.$$

In the case of the B_c^+ system the proportionality between the confinement exchange current and the single quark current operator (11) is lost. The complete scalar pair excitation current operator for the B_c^+ system, to order m^{-2} , has the expression

$$\begin{aligned} \vec{j}_2(C)[B_c^+] = & -e \frac{cr}{6} \left\{ 2 \frac{\vec{p}_c + \vec{p}_c'}{m_c^2} + \frac{\vec{p}_b + \vec{p}_b'}{m_b^2} \right. \\ & \left. + \frac{i}{2} \left[\left(\frac{2}{m_c^2} + \frac{1}{m_b^2} \right) (\vec{\sigma}_c + \vec{\sigma}_b) + \left(\frac{2}{m_c^2} - \frac{1}{m_b^2} \right) (\vec{\sigma}_c - \vec{\sigma}_b) \right] \times \vec{q} \right\}. \end{aligned} \quad (14)$$

The spin dependent part of the corresponding magnetic moment operator takes the form

$$\begin{aligned} \vec{\mu}_2(C)[B_c^+] = & -\frac{cr}{6} m_p \\ & \left\{ \left(\frac{2}{m_c^2} + \frac{1}{m_b^2} \right) (\vec{\sigma}_c + \vec{\sigma}_b) + \left(\frac{2}{m_c^2} - \frac{1}{m_b^2} \right) (\vec{\sigma}_c - \vec{\sigma}_b) \right\} \mu_N. \end{aligned} \quad (15)$$

The first term in this expression contributes to the magnetic moment of the $J > 0$ B_c^+ mesons.

In the B_c^+ system the gluon exchange current operator that arises from excitations of virtual $q\bar{q}$ pair states will contribute to both the magnetic moments and to the spin-flip transition strengths. The complete expression (to order m^{-2}) of this gluon exchange current operator is (in momentum space):

$$\begin{aligned} \vec{j}_2(G)[B_c^+] = & e \frac{8\pi\alpha_s}{9} \left\{ \frac{2}{3} \frac{1}{k_b^2} \left[\frac{\vec{p}_b + \vec{p}_b'}{m_c m_b} + i \left(\frac{\vec{\sigma}_c}{m_c^2} + \frac{\vec{\sigma}_b}{m_c m_b} \right) \times \vec{k}_b \right] \right. \\ & \left. + \frac{1}{3k_c^2} \left[\frac{\vec{p}_c + \vec{p}_c'}{m_c m_b} + i \left(\frac{\vec{\sigma}_c}{m_c m_b} + \frac{\vec{\sigma}_b}{m_b^2} \right) \times \vec{k}_c \right] \right\}. \end{aligned} \quad (16)$$

Here the momentum operators \vec{k}_b and \vec{k}_c denote the fractional momenta delivered to the \bar{b} and c quarks respectively ($\vec{q} = \vec{k}_b + \vec{k}_c$).

The spin dependent part of the magnetic moment operator for the gluon exchange current operator (16) takes the form

$$\vec{\mu}_2(G)[B_c^+] = \frac{\alpha_s m_p}{27 r} \left\{ \left(\frac{2}{m_c^2} + \frac{3}{m_c m_b} + \frac{1}{m_b^2} \right) (\vec{\sigma}_c + \vec{\sigma}_b) \right.$$

$$+ \left(\frac{2}{m_c^2} - \frac{1}{m_c m_b} - \frac{1}{m_b^2} \right) (\vec{\sigma}_c - \vec{\sigma}_b) \Big\} \mu_N. \quad (17)$$

Note that the presence of the spin-flip term in (17) is solely a consequence of the difference in mass of the charm and beauty quarks.

4 Radiative Spin-Flip Transitions

The spin-flip part of the magnetic moment operators considered above may be expressed in the general form

$$\vec{\mu}_{S.F} = \mathcal{M}(\vec{\sigma}_Q - \vec{\sigma}_{\bar{q}}), \quad (18)$$

where \mathcal{M} is the matrix element of the orbital part of the operator for the transition and e is the elementary charge. The width for a radiative spin-flip transition of the form $Q\bar{q}(J=1) \rightarrow Q\bar{q}(J=0)\gamma$ then takes the form

$$\Gamma = \frac{4}{3} \alpha_{em} \frac{M_f}{M_i} \mathcal{M}^2 q^3. \quad (19)$$

Here α_{em} is the fine structure constant, q is the photon momentum in the laboratory frame, and M_i and M_f are the masses of the initial and final states respectively. The matrix element \mathcal{M} is formed of a single quark current term and an exchange current term. These expressions for the heavy quarkonium systems are given explicitly below.

4.1 Spin-flip transitions in the $c\bar{c}$ system

For radiative spin-flip decays of the form $\psi(nS) \rightarrow \eta_c \gamma$ and $\eta'_c(nS) \rightarrow \psi \gamma$ the matrix element (19) \mathcal{M} may be derived from the single quark operator (7) and the exchange current contribution (12) that is associated with the scalar confining interaction. The matrix element \mathcal{M} then takes the form [7]:

$$\mathcal{M} = \frac{1}{3m_c} \{I_1 + I_c\}. \quad (20)$$

The factor $1/3m_c$ arises from the charge factor $2/3$ and the factor $1/2m_c$ in the magnetic moment operator. The dimensionless integrals I_1 and I_c that

arise from the single quark operator (7) and the confining exchange current (12) respectively have the explicit expressions (cf.(8), (13)).

$$I_1 = 4 \int_0^\infty dp p^2 \int_{-1}^1 dz \int_0^\infty dr' r'^2 \int_0^\infty dr r^2 \varphi_f^*(r') \frac{1}{\sqrt{1+v^2}} \left\{ 1 - \frac{1}{3} \left(1 - \frac{1}{\sqrt{1+v^2}} \right) \right\} j_0 \left(r' \sqrt{p^2 + pqz/2 + q^2/16} \right) j_0 \left(r \sqrt{p^2 - pqz/2 + q^2/16} \right) \varphi_i(r), \quad (21)$$

$$I_c = -\frac{c}{m_c} \int_0^\infty dr r^2 \varphi_f^*(r) r \varphi_i(r). \quad (22)$$

Here $v \equiv p/m$. The first of these two integrals reduces to the form (8) (with exception of the factor $2m_p\mu/3m_Q$) in the static limit $v \rightarrow 0$.

Transition	NRIA	RIA	RIA+conf	Exp.
$1^3S_1 \rightarrow 1^1S_0$	2.87 keV	2.18 keV	1.05 keV	1.14 ± 0.39 keV
$2^3S_1 \rightarrow 1^1S_0$	1.54 keV	0.206 keV	1.32 keV	0.78 ± 0.24 keV
$2^3S_1 \rightarrow 2^1S_0$	1.43 keV	1.03 keV	0.14 keV	—
$2^1S_0 \rightarrow 1^3S_1$	0.188 keV	0.469 keV	0.351 keV	—
$3^3S_1 \rightarrow 1^1S_0$	0.795 keV	0.172 keV	0.929 keV	—
$3^3S_1 \rightarrow 2^1S_0$	0.61 keV	0.0753 keV	1.24 keV	—
$3^3S_1 \rightarrow 3^1S_0$	2.32 keV	1.57 keV	0.0124 keV	—
$3^1S_0 \rightarrow 1^3S_1$	0.167 keV	0.228 keV	0.372 keV	—
$3^1S_0 \rightarrow 2^3S_1$	0.0133 keV	0.12 keV	0.233 keV	—

Table 5: Decay widths for the $c\bar{c}$ system. The columns NRIA and RIA contain the results of the non-relativistic and relativistic impulse approximations respectively. The net calculated decay width obtained by combining the relativistic impulse approximation and exchange current contributions is given in the column RIA+conf. The empirical values are from ref.[17]

The calculated decay widths for spin-flip transitions between the S -states of the $c\bar{c}$ system are given in Table 5. In Table 5 the decay width results that are obtained in the non-relativistic and relativistic impulse approximations are also given both in order to facilitate comparison to the results of refs.

[7, 8] and to bring out the significant role of the exchange current contribution. Note that in the numerical calculation the empirical values for the photon momenta have been used in order to obtain the correct phase space factors. This makes a difference only for transitions that involve the J/ψ state, which is somewhat overpredicted by the present model. This issue does not affect the wave functions, which were calculated without account of the hyperfine terms of order v^2/c^2 , which were treated in lowest order perturbation theory.

The results in Table 5 show that the non-relativistic impulse approximation overestimates the rate for $J/\psi \rightarrow \eta_c \gamma$ by a factor ~ 3 as has been noted earlier [7, 8]. By employing the unapproximated magnetic moment operator (7) this overestimate is reduced to a factor ~ 2 . Agreement with the empirical value is achieved only by taking into account the exchange current contribution. In the case of the transition $\psi(2S) \rightarrow \eta_c \gamma$ the impulse approximation underestimates the empirical decay width by a large factor. For this transition the exchange current contribution is the dominant one. The net calculated result falls only slightly above the upper limit of the uncertainty range of the present empirical result. There is no instance, where the non-relativistic impulse approximation result is close to either the empirical value, or to the net calculated result. This feature emphasizes the point that the M1 transitions are peculiarly sensitive to the strength and form of the confining interaction through the associated exchange current. The ultimate reason for this sensitivity is of course the fact that there is destructive interference between the different contributions to the transition amplitude. Those calculated widths, which are exceptionally small therefore also have the largest theoretical uncertainty, as even tiny modifications in the model parameters could cause large relative changes.

4.2 Spin-flip transitions in the $b\bar{b}$ system

For radiative spin-flip transitions in the $b\bar{b}$ system the matrix element \mathcal{M} in (19) takes the form :

$$\mathcal{M} = -\frac{1}{6m_b} \{I_1 + I_c\}. \quad (23)$$

The factor $-1/6m_b$ arises from the charge factor $-1/3$ and the factor $1/2m_b$ in the magnetic moment operator. The dimensionless integrals I_1 and I_c are

defined as in eqs. (21), (22).

The calculated decay rates reveal that even in the case of the $b\bar{b}$ system the non-relativistic impulse approximation is unreliable, except in the case, where the initial and final states have the same degree of excitation. In those cases it leads to overestimates of the net calculated decay rates by factors ~ 2 . The exchange current contribution is large for all these spin-flip transitions, and in fact the dominant contribution for transitions between states with different excitation number.

Transition	NRIA	RIA	RIA + conf
$1^3S_1 \rightarrow 1^1S_0$	23.4 eV	21.2 eV	18.9 eV
$2^3S_1 \rightarrow 1^1S_0$	3.45 eV	2.02 eV	0.215 eV
$2^3S_1 \rightarrow 2^1S_0$	4.09 eV	3.70 eV	2.77 eV
$2^1S_0 \rightarrow 1^3S_1$	0.74 eV	2.25 eV	0.0069 eV
$3^3S_1 \rightarrow 1^1S_0$	2.82 eV	3.56 eV	0.126 eV
$3^3S_1 \rightarrow 2^1S_0$	1.41 eV	0.35 eV	1.09 eV
$3^3S_1 \rightarrow 3^1S_0$	2.06 eV	1.83 eV	1.32 eV
$3^1S_0 \rightarrow 1^3S_1$	1.15 eV	3.50 eV	0.347 eV
$3^1S_0 \rightarrow 2^3S_1$	0.296 eV	0.529 eV	0.253 eV

Table 6: Decay widths for the $b\bar{b}$ system. The columns NRIA and RIA contain the results of the non-relativistic and relativistic impulse approximations respectively. The net calculated decay width obtained by combining the relativistic impulse approximation and exchange current contributions is given in the column RIA+conf.

4.3 Spin-flip transitions in the B_c^+ system

The magnetic moment of the 3S_1 ground state of the B_c^+ system that is obtained from the expression 10 is

$$\mu(RIA) = \frac{4}{3}m_p\mu_N \int_0^\infty dp p^2 \int_{-1}^1 dz$$

$$\int_0^\infty dr' r'^2 \int_0^\infty dr r^2 \varphi(r') \left\{ \frac{2}{m_c \sqrt{1 + \vec{v}_c^2}} \left\{ 1 - \frac{1}{3} \left(1 - \frac{1}{\sqrt{1 + \vec{v}_c^2}} \right) \right\} \right\}$$

$$+ \left\{ \frac{1}{m_b \sqrt{1 + \vec{v}_b^2}} \left\{ 1 - \frac{1}{3} \left(1 - \frac{1}{\sqrt{1 + \vec{v}_b^2}} \right) \right\} \right\} j_0(r'p) j_0(rp) \varphi(r). \quad (24)$$

Here $\varphi(r)$ is the radial wave function for the 3S_1 state. If the velocity dependent “relativistic” correction terms are dropped from this expression it reduces to the static quark model result

$$\mu(IA) \simeq \frac{1}{3} \left\{ \frac{2m_p}{m_c} + \frac{m_p}{m_b} \right\} \mu_N. \quad (25)$$

With the quark mass values in Table 1 the static approximation value is $0.49 \mu_N$. When calculated from the unapproximated expression (24) this result is reduced to $0.420 \mu_N$.

The exchange current contributions to this magnetic moment value is obtained from the spin-symmetric terms in the exchange magnetic moment expressions 15 and 17 for the confining and gluon exchange interactions respectively. The explicit expressions for these corrections are

$$\mu(C) = -\frac{m_p}{3} c \left\{ \frac{2}{m_c^2} + \frac{1}{m_b^2} \right\} \int_0^\infty dr r^3 \varphi^2(r) \mu_N, \quad (26)$$

$$\mu(G) = \frac{2\alpha_s}{27} m_p \left\{ \frac{2}{m_c^2} + \frac{3}{m_c m_b} + \frac{1}{m_b^2} \right\} \int_0^\infty dr r \varphi^2(r) \mu_N. \quad (27)$$

Numerical evaluation of these two expressions give the results $\mu(C) = -0.10 \mu_N$ and $\mu(G) = 0.036 \mu_N$ respectively. When these values are added to the impulse approximation result $0.420 \mu_N$ the net calculated magnetic moment becomes $0.35 \mu_N$. The static quark model value therefore is expected to represent an overestimate of the net magnetic moment value of about 23 %. This conclusion is in line with estimates of the exchange current and relativistic corrections to the static quark model predictions of the magnetic moments of the baryons, but in that case the situation is more complex because of the possibly substantial exchange current contributions associated with flavor dependent meson exchange interactions [15, 18].

The spin-flip transitions in the B_c^+ systems differ from those of the $c\bar{c}$ and $b\bar{b}$ systems in that they also obtain contributions from the gluon exchange

magnetic moment operator (17). This contribution turns out in most cases to be weak in comparison with that from the exchange magnetic moment operator that is due to the confining interaction (15). This is shown in Table 7, where the calculated decay widths for the spin-flip transitions between the (predicted) S -states of the B_c^+ system are given with and without inclusion of the gluon exchange current contribution. The role of the gluon exchange current contribution is in every instance to increase the net exchange current contribution.

In the non-relativistic impulse approximation we obtain spin-flip transition decay widths that are close to those obtained in ref.[12]. As shown by the comparison between the calculated decay widths that are obtained in the non-relativistic impulse approximation with the values obtained with the complete Dirac magnetic moment operator, the former approximation leads to overestimates by factors, which are typically larger than ~ 2 .

The role of the exchange current contribution is predicted to be large for the spin-flip transitions in the B_c^+ system. The net calculated result typically differs from that obtained in the relativistic impulse approximation by an order of magnitude, the only exceptions being the transitions between states with the same excitation number.

Transition	NRIA	RIA	RIA + conf	RIA +conf + gluon
$1^3S_1 \rightarrow 1^1S_0$	138 eV	91.4 eV	42.5 eV	51.4 eV
$2^3S_1 \rightarrow 1^1S_0$	62.1 eV	375 eV	5.40 eV	46.1 eV
$2^3S_1 \rightarrow 2^1S_0$	43.0 eV	27.0 eV	3.08 eV	3.94 eV
$2^1S_0 \rightarrow 1^3S_1$	12.6 eV	249 eV	0.688 eV	15.6 eV
$3^3S_1 \rightarrow 1^1S_0$	38.5 eV	145 eV	30.5 eV	129 eV
$3^3S_1 \rightarrow 2^1S_0$	21.3 eV	110 eV	56.9 eV	85.7 eV
$3^3S_1 \rightarrow 3^1S_0$	27.4 eV	15.8 eV	0.0145 eV	0.0758 eV
$3^1S_0 \rightarrow 1^3S_1$	14.3 eV	107 eV	17.8 eV	80.8 eV
$3^1S_0 \rightarrow 2^3S_1$	3.00 eV	66.5 eV	23.8 eV	35.8 eV

Table 7: Decay widths for the B_c^+ system

5 Discussion

The present results suggest that the exchange current operator that is associated with the scalar confining interaction through current conservation gives a crucial contribution to the decay rates for radiative spin-flip transitions in heavy quarkonia. In most cases it interferes destructively with the matrix element of the single quark magnetic moment operator. As a consequence the value for these decay rates obtained in the impulse approximation differs from the net calculated decay rate by large factors.

The results support the observation made in refs. [7, 8] that the relativistic corrections to the single quark magnetic moment operator are of significant magnitude, although with the present unapproximated treatment of the relativistic magnetic moment operator, these relativistic corrections are moderated somewhat.

The most important exchange current operator is that associated with the scalar confining interaction. The gluon exchange current only contributes a small additional correction to the radiative decays of the B_c+ system. Both these exchange current operators involve excitation of intermediate virtual $q\bar{q}$ pairs. The exchange current corrections therefore do involve the negative energy components of the quark spinors. That such negative energy components are numerically significant has also been pointed out in ref.[9], although in a quite different approach to the problem, based on an instantaneous approximation to the Bethe-Salpeter equation. The present Schrödinger equation approach with exchange currents, pioneered in refs.[7, 8], would appear somewhat more transparent, and as shown above appears to yield decay rates for the spin-flip transitions of heavy quarkonia, that compare more favorably with extant empirical values. The present Schrödinger equation approach may be derived from the Bethe-Salpeter equation by means of a three-dimensional quasipotential reduction in the adiabatic limit [19].

The present results suggest that the exchange current operator that is associated with the confining interaction should play an important role in radiative transitions of heavy vector mesons to heavy pseudoscalar mesons, in particular the transitions $D^* \rightarrow D\gamma$, $D_s^* \rightarrow D_s\gamma$ and $B^* \rightarrow B\gamma$.

Acknowledgments

DOR thanks Dr. Håkan Snellman for drawing attention to the M1 transitions in heavy quarkonia. TL and CN thank the Finnish Society of Sciences and Letters for support. Research supported in part by the Academy of Finland under contract 34081.

References

- [1] S. Godfrey and N. Isgur, Phys. Rev. **D32** (1985) 189
- [2] E.J. Eichten and C. Quigg, Phys. Rev. **D52** (1995) 1726
- [3] G.S. Bali, K. Schilling and A. Wachter, eprint hep-ph/9611226
- [4] G.S. Bali, K. Schilling and A. Wachter, Phys. Rev. **D56** (1997) 2566
- [5] C. T. H. Davies et al., Phys. Lett. **B345** (1996) 42
- [6] C.T.H. Davies et al. Phys. Rev. **D56** (1997) 2755-2765
- [7] H. Grotch, D.A. Owen and K.J. Sebastian, Phys. Rev. **D30** (1984) 1924
- [8] X. Zhang, K.J. Sebastian and H. Grotch, Phys. Rev. **D44** (1991) 1606
D30:1924, 1984
- [9] J. Linde and H. Snellman, Nucl. Phys. **A619** (1997) 346 hep-ph/9703383
- [10] D. Gromes Phys. Lett **B202** (1988) 262
- [11] F. Abe et al. (CDF Collaboration) Phys. Rev. Lett. **81** (1998) 2432
- [12] E.J. Eichten and C. Quigg, Phys. Rev. **D49** (1994) 5845
- [13] W. Buchmüller and S.-H. H. Tye, Phys. Rev. **D24** (1981) 132
- [14] T. Barnes, Third Workshop on the Tau-Charm Factory, J. Kirkby and R. Kirkby, Eds., Editions Frontieres, Gif-sur-Yvette (1994) 411
- [15] K. Dannbom et al. Nucl. Phys. **A616** (1996) 555
- [16] J. L. Friar, Mesons in Nuclei, M. Rho and D. Wilkinson, Eds., North-Holland Publ. Co., Amsterdam (1979), Vol.2, 595

- [17] C. Caso et al. (Particle Dat Group), Eur. Phys. J. **C3** (1998) 1
- [18] C. Helminen, eprint hep-ph/9711252
- [19] F. Coester and D. O. Riska, Ann. Phys. **234** (1994) 511